Intrinsic Circular Polarization in Centrosymmetric Stacks of Transition-Metal Dichalcogenide Compounds

Qihang Liu,* Xiuwen Zhang, and Alex Zunger†
University of Colorado, Boulder, Colorado 80309, USA

(Received 21 June 2014; revised manuscript received 28 January 2015; published 27 February 2015)

The circular polarization (CP) that the photoluminescence inherits from the excitation source in n monolayers of transition-metal dichalcogenides $(MX_2)_n$ has been previously explained as a special feature of *odd* values of n, where the inversion symmetry is absent. This "valley polarization" effect results from the fact that, in the absence of inversion symmetry, charge carriers in different band valleys could be selectively excited by different circular polarized light. Although several experiments observed CP in centrosymmetric MX_2 systems, e.g., for bilayer MX_2, they were dismissed as being due to some extrinsic sample irregularities. Here we show that also for $n =$ even, where inversion symmetry is present and valley polarization physics is strictly absent, such intrinsic selectivity in CP is to be expected on the basis of fundamental spin-orbit physics. First-principles calculations of CP predict significant polarization for $n = 2$ bilayers: from 69% in MoS_2 to 93% in WS_2. This realization could broaden the range of materials to be considered as CP sources.

DOI: 10.1103/PhysRevLett.114.087402 PACS numbers: 78.55.-m, 72.25.Fe, 75.70.Tj, 78.67.De

The quest for a system manifesting a single type of circular polarized light, left handed (LH, or σ_+) or right handed (RH, or σ_-), has been motivated by its promising application in fields such as spin-Hall effect and quantum computation [1–6]. The magnitude of the effect is conveniently measured by circular polarization (CP), i.e., the anisotropy of circular polarized luminescence [7],

$$\rho = \frac{I(\sigma_+) - I(\sigma_-)}{I(\sigma_+) + I(\sigma_-)}, \tag{1}$$

where $I(\sigma_+)$ and $I(\sigma_-)$ denote the intensity of the LH and RH polarized luminescence, respectively. One approach to the creation of CP is the utilization of spin-orbit-induced CP [6] in which spin-orbit coupling (SOC) in low-symmetry bulk solids creates spin splitting (the Dresselhaus [8] and Rashba [9] effects), leading to spin-sensitive absorption and thus polarized luminescence. Another approach to achieving large ρ is the creation of valley-selective CP [10]. Here absorption selects the wave function character that can couple with the circular polarized light, and SOC is not needed to produce the effect. An example is $n =$ odd monolayers of 2H-stacking transition-metal dichalcogenides $(MX_2)_n$ (with $M =$ Mo, W, $X =$ S, Se), having two valleys K and $-K$ with equal energies located at the corners of their hexagonal Brillouin zone. For a single monolayer $n = 1$, the lowest energy transition is momentum-space direct at the wave vectors K and $-K$ and the wave functions of the valence band maximum $\psi_v^{(n=1)}(K) = \chi_+$ and $\psi_v^{(n=1)}(-K) = \chi_-$ have pure LH or RH characters, respectively. As a result, σ_+ excitation can excite the valence electrons at the K valley but no electrons at the $-K$ valley, while σ_- can only excite valence electrons at the $-K$ valley but none of those at the K valley. Such valley-contrasting CP leads to valleytronics, a parallel concept of spintronics, with the emergence of interesting phenomena such as valley-Hall effect [11,12]. However, the limitation to noncentrosymmetric systems both in the spin-orbit-induced CP and in the valleytronics-induced CP poses a restriction on material selection for achieving CP.

For a bilayer MX_2 ($n = 2$) the lowest energy transition is momentum indirect, whereas the direct transition at the K and $-K$ valley is higher in energy, but the exciton emission from these direct states is still rather strong [13]. More surprisingly, highly selective CP (up to $\rho = 80\%$) has been observed for this direct transition in bilayer MX_2 that has inversion symmetry [7,13–16]. Since this fact goes against the generally accepted expectation that valley-induced CP should be intrinsically absent in centrosymmetric (such as even n) materials, various *extrinsic* scenarios were offered to rationalize this unusual observation, such as substrate charging, low-quality sample, heating effects, etc. [7,15,16].

Recently, Gong *et al.* [17] discussed the magnetoelectric effects of bilayer MX_2 using $k \cdot p$ and the tight-binding method. They have argued that because the interlayer coupling is weak, bilayers will inherit most of the spin-valley physics of monolayers, named "spin-layer locking." In this Letter, we focus instead on spin-orbit physics as local effect, building on the recent realization [18] that SOC-induced spin polarization can exist not only when inversion symmetry is absent, but also in systems where inversion symmetry is present (i.e., globally centrosymmetric systems) while its individual sectors (e.g., monolayers) lack inversion. We show that such "hidden spin

polarization" can lead to CP for $n =$ even values of $(MX_2)_n$. This is illustrated in Fig. 1, showing our first-principles calculated ρ for the emission from the direct band states at the K and $-K$ valley as a function of the number of monolayers n in $(MX_2)_n$, reaching asymptotically the bulk value for a large n. We see that the CP decreases monotonically with increasing n and the results of a fixed material lie on one curve without odd-even oscillations, in contrast to the expectation based on valley symmetries [10,15,16]. By recognizing that the spin-orbit physics can induce CP and that this effect is no longer limited to low-symmetry noncentrosymmetric structures, our finding could broaden the range of materials to be considered as spintronic CP sources.

Local spin polarization in each monolayer within bilayer MX_2.—This intrinsic CP in centrosymmetric systems originating from hidden spin polarization can be illustrated for bilayer $n = 2$ in $(MX_2)_n$, where two inversion-asymmetric individual MX_2 layers α and β ("sectors" in general) carry opposite local spin polarization. In bilayer MX_2, a monolayer MX_2 named β is introduced to form an inversion partner of layer α. The corresponding energy bands must be spin degenerate due to the combination of inversion symmetry and time-reversal symmetry. However, such global k-space compensation of spins does not occur in a point-by-point fashion in real space, i.e., on each MX_2 layer. Using density functional theory calculation implemented by VASP [19] with a projected augmented wave pseudopotential [20], we can project the twofold degenerate wave functions with plane wave expansion on the spin and orbital basis (spherical harmonics) of each atomic site. For the K valley of the top valence band ($V1$),

$$\psi_v^{(n=2)}(K,\uparrow) = \sum_{l,m,i} C_{l,m,i,\uparrow}|l,m,i\rangle \otimes |\uparrow\rangle,$$
$$\psi_v^{(n=2)}(K,\downarrow) = \sum_{l,m,i} C_{l,m,i,\downarrow}|l,m,i\rangle \otimes |\downarrow\rangle, \quad (2)$$

with the module squared expansion coefficient

$$|C_{i,l,m,\eta}|^2 = \langle \psi_v^{(n=2)}(K,\eta)|(s_z \otimes |l,m,i\rangle\langle l,m,i|)|\psi_v^{(n=2)}(K,\eta)\rangle, \quad (3)$$

where $\psi_v^{(n=2)}(K,\eta)$ is the hole state of bilayer MX_2, $|l,m,i\rangle$ is the orbital angular momentum eigenstate centered about the ith atomic site, $s_z = (\hbar/2)\sigma_z$ is the spin operator, and η denotes spin. Note that at the K and $-K$ valley, s_z is a good quantum number with two spin eigenstates $|\uparrow\rangle$ and $|\downarrow\rangle$. By summing $C_{i,l,m,\eta}$ separately for layer α and layer β (each containing 3 atomic sites in a unit cell), we find that for the K valley of $V1$ in bilayers of MoS_2, $MoSe_2$, WS_2, and WSe_2 the spin polarization localized on layer α, $S = \sum_{l,m,i\in\alpha}(|C_{i,l,m,\uparrow}|^2 - |C_{i,l,m,\downarrow}|^2)$, is 0.83, 0.90, 0.97, and 0.95 (out of plane, in the unit of $\hbar/2$), respectively, and the local spin polarization on layer β has exactly the same magnitude but opposite direction. Thus, despite the global inversion of the $n = 2$ structure, each individual layer experiences a nonzero local spin polarization S in real space, "hidden" by the presence of the counterpart on the other layer. We next show that in such even-layer stacks of $(MX_2)_n$ the hidden spin polarizations induce CP as an intrinsic part of the fundamental physics even without any sample irregularities.

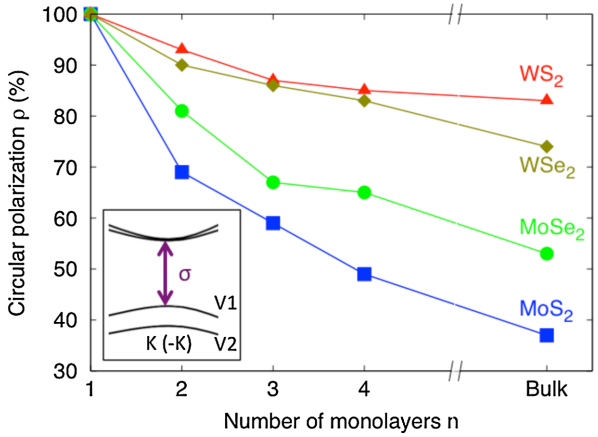

FIG. 1 (color online). Calculated circular polarization ρ for different $(MX_2)_n$ materials as a function of the number of monolayers n. ρ corresponds to the direct states at the K and $-K$ valley no matter whether they correspond to the lowest-energy excitation (as in $n = 1$) or higher-energy resonant excitation (as in $n > 1$) of circular polarized light. The inset shows a schematic band structure of bilayer MX_2. The results by σ_+ and σ_- excitation have the same magnitude but opposite sign.

Photoluminescence process leading to circular polarization.—To calculate the CP of Eq. (1) that involves an emission experiment, we need a model of what happens to the photoexcited carriers before emission. Taking bilayer MX_2 as an example, we next consider the absorption, relaxation, and emission process, as illustrated in Fig. 2. The splitting between the top two valence bands $V1$ and $V2$ at K and $-K$ is due to SOC-induced spin splitting and the interlayer coupling. Here we consider resonant excitation (the incident photon energy equals the direct band gap at K or $-K$), in which only $V1$ is of interest.

Interband absorption is described by the up arrow indicated as (1) in Fig. 2(a). It involves promoting an electron from a valence band eigenstate of Eq. (2) momentum directly into a conduction band eigenstate, evaluated by the transition matrix element $\mathcal{P}_\pm = \langle \psi_c|p_x \pm ip_y|\psi_v\rangle$, where $\boldsymbol{p}$ is the momentum operator. By calculating the transition matrix element for circular polarized light, say σ_+, we find that unlike the case of one monolayer in which absorption is valley contrasting, in bilayer MX_2 the K and $-K$ valley have the same absorption, consistent with the presence of global inversion symmetry [10]. However, our present density functional theory calculations show that the two degenerate spin states in Eq. (2) have different nonzero absorption magnitude, leading to a net spin of the excited

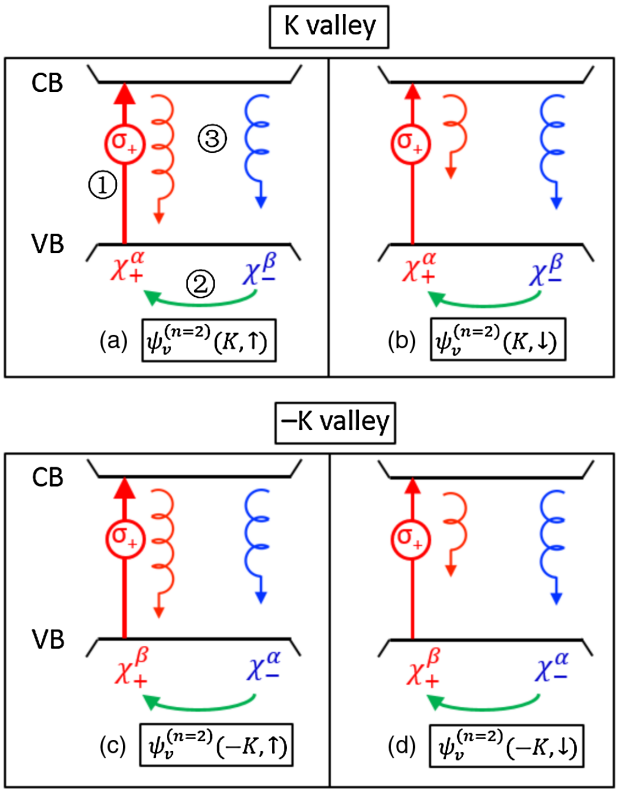

FIG. 2 (color online). Schematic diagram of photoluminescence process at the K and $-K$ valley in bilayer MX_2. Four degenerate valence band (VB) states described in Eqs. (4) and (5), i.e., (a) $\psi_v^{(n=2)}(K,\uparrow)$, (b) $\psi_v^{(n=2)}(K,\downarrow)$, (c) $\psi_v^{(n=2)}(-K,\uparrow)$, and (d) $\psi_v^{(n=2)}(-K,\downarrow)$, are shown with χ_+ (red) and χ_- (blue) denoting LH and RH orbitals of the valence states, respectively. Taking (a) as an example, three steps in photoluminescence are indicated. (1) Absorption by a resonant σ_+ excitation. The red arrow indicates that the excitation promotes electrons with χ_+ character into conduction band (CB). (2) Intrastate relaxation denoted by green arrows. (3) Radiative recombination filling the holes of the VB state. The red and blue curled arrows denote σ_+ and σ_- emission, respectively, with the lengths representing the relative intensity of emission regarding $C_{\mathrm{maj}} > C_{\mathrm{min}}$.

electrons. To interpret this effect and its impact on CP, we reconsider the valence band eigenstates of the bilayer system in Eq. (2) expanded in terms of single monolayer eigenstates, $\psi_v^{(n=1)}(K) = \chi_+$ and $\psi_v^{(n=1)}(-K) = \chi_-$, having pure LH or RH characters, respectively. We approximate the wave function of bilayer MX_2 at the K valley as an expansion in terms of the α layer ($\chi_+^{(\alpha)}$) and the $-K$ valley of the β layer ($\chi_-^{(\beta)}$) eigenstates, written as

$$\psi_v^{(n=2)}(K,\uparrow) = (C_{\alpha,\uparrow}\chi_+^{(\alpha)} + C_{\beta,\uparrow}\chi_-^{(\beta)}) \otimes |\uparrow\rangle,$$
$$\psi_v^{(n=2)}(K,\downarrow) = (C_{\alpha,\downarrow}\chi_+^{(\alpha)} + C_{\beta,\downarrow}\chi_-^{(\beta)}) \otimes |\downarrow\rangle, \quad (4)$$

where the module squared coefficient is $|C_{\alpha(\beta),\eta}|^2 = \sum_{l,m,i\in\alpha(\beta)} |C_{i,l,m,\eta}|^2$, and $C_{\alpha,\uparrow} = C_{\beta,\downarrow} = C_{\mathrm{maj}}$, $C_{\beta,\uparrow} = C_{\alpha,\downarrow} = C_{\mathrm{min}}$ denote the majority (maj) and minority (min) component for each valence spin state. The subscript $+$ $(-)$ denotes a pure LH (RH) wave function component. The wave functions of $V1$ at the $-K$ valley is just related to those at the K valley by time reversal

$$\psi_v^{(n=2)}(-K,\uparrow) = (C_{\mathrm{maj}}\chi_+^{(\beta)} + C_{\mathrm{min}}\chi_-^{(\alpha)}) \otimes |\uparrow\rangle,$$
$$\psi_v^{(n=2)}(-K,\downarrow) = (C_{\mathrm{min}}\chi_+^{(\beta)} + C_{\mathrm{maj}}\chi_-^{(\alpha)}) \otimes |\downarrow\rangle. \quad (5)$$

We have tested the approximation of expanding $n = 2$ just by the two $n = 1$ eigenstates by comparing the calculated ratio of transition matrix elements $\mathcal{P}_+(K,\uparrow)/\mathcal{P}_+(K,\downarrow)$ of the corresponding spin states with the initial plane wave expansion via first-principles calculation, and find it in good agreement with $|C_{\mathrm{maj}}|^2/|C_{\mathrm{min}}|^2$ from Eqs. (4) and (5), indicating the validity of our wave function decomposition onto the monolayer basis.

Unlike the case of one monolayer in which $\psi_v^{(n=1)}(\pm K)$ have pure LH or RH components (χ_+ and χ_-), the four valence states of bilayer MX_2, described by Eqs. (4) and (5), have both χ_+ and χ_- components. Therefore, for σ_+ resonant excitation, only the electrons with $\chi_+^{(\alpha)}$ character at the K valley and the electrons with $\chi_+^{(\beta)}$ character at the $-K$ valley are excited (χ_- components have no contribution to the transition matrix element), as shown in Fig. 2 by step (1). Note that for $\psi_v^{(n=2)}(K,\uparrow)$ and $\psi_v^{(n=2)}(-K,\uparrow)$ eigenstates [Figs. 2(a) and 2(c)], the excited component is the majority term (proportional to $|C_{\mathrm{maj}}|^2$) with up spin $|\uparrow\rangle$, while for $\psi_v^{(n=2)}(K,\downarrow)$ and $\psi_v^{(n=2)}(-K,\downarrow)$ states [Figs. 2(b) and 2(d)], the excited component is the minority term (proportional to $|C_{\mathrm{min}}|^2$) with down spin $|\downarrow\rangle$. As a result, the excited electrons have a net up spin that equals the local spin polarization on the α layer at the K valley (or β layer at $-K$) derived from Eqs. (4) and (5), $S = [(|C_{\mathrm{maj}}|^2 - |C_{\mathrm{min}}|^2)/(|C_{\mathrm{maj}}|^2 + |C_{\mathrm{min}}|^2)]$, creating simultaneously equivalent holes with the same net spin.

Following excitation, relaxation mechanisms might redistribute the photogenerated LH and RH holes, thereby reducing the polarization anisotropy ρ. The observed ρ for monolayer MoS_2 has been as large as 100% [7], suggesting ineffective mixture of photogenerated LH and RH holes caused by intervalley relaxation and thus excellent retention of the valley-contrasting circular absorption. In bilayer MX_2, the dominated relaxation route considered here is illustrated by the green arrow labeled step (2) in Fig. 2(a). For the σ_+ excitation, all of the promoted electrons have χ_+ character, leaving the excited state with a different LH/RH ratio compared with the ground state. Consequently, the LH and RH components tend to redistribute within the same valence eigenstate to retain the ground state ($\chi_- \rightarrow \chi_+$). Such intrastate relaxation could happen much faster than the electron-hole recombination because of the imbalance excitation between χ_+ and χ_- components and the lack of an effective barrier to suppress the spin-conserved relaxation. Three kinds of other relaxation channels that could

mix LH and RH components and thus affect ρ are also considered. We assume the relaxation time with spin flip much slower, and the relaxation time with spin conserving much faster, than the electron-hole recombination time, with the details listed in Supplemental Material [21].

As indicated by red and blue curled arrows [step (3)], the radiative recombination fills the holes with χ_+ and χ_- characters of a valence band, leading to σ_+ and σ_- luminescence, respectively. In Figs. 2(a) and 2(c), the excited χ_+ component is majority, so the total emission is larger than that in Figs. 2(b) and 2(d), in which the excited χ_+ component is minority. Note that the magnitude of σ_+ and σ_- emission in each state reflects the comparison of χ_+ and χ_- components. The Supplemental Material considers the matrix elements (i.e., electric dipole) of interband absorption under resonant excitation [Eqs. (S1)–(S6) [21]]. After relaxation and emission processes take place [Eqs. (S7)–(S11) [21]], the expression of the total CP defined by Eq. (1) emerges [21]:

$$\rho = \left(\frac{|C_{\mathrm{maj}}|^2 - |C_{\mathrm{min}}|^2}{|C_{\mathrm{maj}}|^2 + |C_{\mathrm{min}}|^2}\right)^2. \tag{6}$$

Similarly, we can get exactly opposite ρ by using σ_- resonant excitation (see Fig. S1 [21]). From Eq. (6) we find that the polarization anisotropy ρ is closely related to S: if a centrosymmetric material has local spin polarization on each inversion-asymmetric sector, we can find nonzero CP following excitation of circular polarized light, as all the MX_2 bilayers shown in Fig. 1.

The calculated CP [Eq. (6)] refers to the direct transition at the K and $-K$ valley, in which there is a nonradiative electron relaxation from the excited conduction band edge to the lower conduction band minimum. This process naturally causes a reduction of intensity of the photoluminescence from the excited conduction band, which may in turn contribute to some uncertainty in its measurement (and thus could be responsible for some of the deviation with theory). Recent experiments [13,29] show, however, that although the photoluminescence of the direct band gap energy at the K ($-K$) valley in the bilayer has a much lower intensity than that in the monolayer case (less than 10%), the intensity is still sufficient to measure the CP. Note that the central quantity here—the ratio between emission intensities at different polarizations [Eq. (1)]—need not be affected by the fundamental transition being direct or indirect.

Progression of CP from $n = 1$ to bulk MX_2.—From the above discussion we note that the CP of bilayer MX_2 is directly related to the spin polarization localized on each layer, rather than the global inversion symmetry. This dependence provides us the route to evaluate CP for all $(MX_2)_n$ stacks by straightforwardly calculating the ratio of LH/RH components of the valence band wave functions expanded by monolayer basis. For the $2H$-MX_2 stacking pattern, the K ($-K$) valley of each monolayer in $(MX_2)_n$ has a pure LH or RH component alternatively, depending on the odd-even parity of the layer index. When $n > 1$, The band edges of $(MX_2)_n$ at the K and $-K$ valley, whether degenerate or nondegenerate, no longer have a certain helicity, but a mixture of LH and RH characters from different layers, leading to the reduction of CP away from the case of the monolayer. If the orbital part of (one of) the valence band wave function at the K or $-K$ valley of $(MX_2)_n$ is written as

$$\psi_v = C_1\chi_+^{(1)} + C_2\chi_-^{(2)} + C_3\chi_+^{(3)} + \cdots + C_n\chi_{+/-}^{(n)}, \tag{7}$$

where $C_i (i = 1, 2, \ldots, n)$ is the coefficient of the LH or RH component from the ith layer, we can thus obtain the corresponding theoretical circular polarization by resonant excitation:

$$\rho = \left(\frac{\sum_n (-1)^{n-1}|c_n|^2}{\sum_n |c_n|^2}\right)^2. \tag{8}$$

Note that although the spin part is not included to calculate the CP, it plays a crucial role for the spin-conserving intrastate relaxation and the prevention of spin-flip relaxation. Contrasting with the conventional understanding that the CP should oscillate with odd-even layers due to the absence or presence of inversion symmetry, we found a decreasing polarization ratio with n, as shown in Fig. 1. The occurrence of a regular decrease of the CP reflects the reduction in the spin polarization piece localized on each layer as the number of layers n increases, a decrease caused by the larger mixture of LH and RH components. In addition, all of the $(WX_2)_n$ stacks have larger ρ than that of $(MoX_2)_n$ due to the larger SOC of the W atom. All of the CP curves reveal an asymptotic behavior to the bulk value. This is because starting from $n = 1$, in which the valence states have a pure LH or RH component, the ratio LH/RH tends to saturate as n increases.

Such a trend is confirmed by a recent experiment on few-layer 2H-MoS_2 [29], which also exhibits a decreasing dependence on layer number with saturation, indicating a good agreement with our prediction except for the starting point of CP in the monolayer (about 58%, possibly because of the sample quality). This agreement also suggested that the formation of exciton states, not considered in this work, might not significantly change the calculated CP. Some other experiments also detected nonzero polarized luminescence ρ_{expt} of MX_2 bilayers, but smaller than our calculated theoretical limit (e.g., 14% lower for bilayer WS_2 [13]). We list the possible reasons in the Supplemental Material [21]. Furthermore, because of the local spin on each MX_2 layer, the CPs range from 37% (MoS_2) to 83% (WS_2) even for 2H-stacking *bulk* MX_2 crystal. Recently, the hidden spin polarization effect in bulk WSe_2 has been observed experimentally by spin- and angle-resolved photoemission spectroscopy [30], revealing large layer-dependent local spin polarization. Therefore, we expect the

intrinsic CP in centrosymmetric bulk MX_2 to be realized by upcoming measurements.

Dependence of ρ on the interlayer distance and material design for larger CP.—The dependence of ρ on the interlayer distance for different bilayer MX_2 compounds is shown in Fig. S2 [21]. The curves clearly exhibit that the intrinsic CP is enhanced as the interlayer separation increases, which could be achieved by tensile strain along the stacking direction or within the two-dimensional plane [31]. At the equilibrium separation, our calculated CP is 69% for MoS_2, 81% for $MoSe_2$, 90% for WSe_2, and 93% for WS_2 [32]. Furthermore, when the interlayer distance of the MX_2 bilayer exceeds 4 Å, the coupling between the α and β layer becomes negligible, implying perfect local spin polarization. As a result, the CP approaches the monolayer limit $\rho = 1$ when the interlayer distance is large enough.

Using the understanding of hidden spin polarization, we design a heterostructure with larger CP by intercalating bilayer BN as an inert medium into bilayer $MoSe_2$ (see Supplemental Material [21]). Such sandwiched structures, having both optimized polarization anisotropy $\rho \approx 1$ and large photoluminescence intensity due to their direct band gap, could be good platforms to realize intrinsic CP in a centrosymmetric system by the current synthesis technology [33,34].

In summary, by using first-principles calculations, we demystify the occurrence of intrinsic CP, accessed by direct interband transition at the K and $-K$ valley, in centrosymmetric layer stacks made of individually noncentrosymmetric layers, such as $n = \text{even}(MX_2)_n$. The intrinsic CP decreases monotonically with increasing n, in sharp contrast with the conventional expectation of odd-even oscillations based on valley symmetries. Such polarization anisotropy results from hidden spin polarization that is localized on each MX_2 layer. Our finding is expected to broaden the material selection that is currently limited to noncentrosymmetric systems for achieving CP and related phenomena and provide new possibilities for the manipulation of spin in the field of spintronics and optoelectronics.

We are grateful for the good discussions with Yu Ye from UC Berkeley, Yang Song from Rochester University, Xiaobo Yin from University of Colorado, and helpful codes for the calculation of transition matrix elements from Kanber Lam, Northwestern University. This work was supported by NSF Grant No. DMREF-13-34170. This work used the Extreme Science and Engineering Discovery Environment (XSEDE), which is supported by National Science Foundation Grant No. ACI-1053575.

*qihang.liu85@gmail.com
†alex.zunger@gmail.com

[1] A. Crepaldi *et al.*, Phys. Rev. B **89**, 125408 (2014).
[2] T. D. Nguyen, E. Ehrenfreund, and Z. V. Vardeny, Science **337**, 204 (2012).
[3] V. L. Korenev, I. A. Akimov, S. V. Zaitsev, V. F. Sapega, L. Langer, D. R. Yakovlev, Yu. A. Danilov, and M. Bayer, Nat. Commun. **3**, 959 (2012).
[4] M. Ghali, K. Ohtani, Y. Ohno, and H. Ohno, Nat. Commun. **3**, 661 (2012).
[5] J. Wunderlich, B. Kaestner, J. Sinova, and T. Jungwirth, Phys. Rev. Lett. **94**, 047204 (2005).
[6] F. Meier and B. P. Zakharchenya, *Optical Orientation* (Elsevier Science, New York, 1984).
[7] K. F. Mak, K. He, J. Shan, and T. F. Heinz, Nat. Nanotechnol. **7**, 494 (2012).
[8] G. Dresselhaus, Phys. Rev. **100**, 580 (1955).
[9] E. I. Rashba, Sov. Phys. Solid State **2**, 1109 (1960).
[10] W. Yao, D. Xiao, and Q. Niu, Phys. Rev. B **77**, 235406 (2008).
[11] D. Xiao, G.-B. Liu, W. Feng, X. Xu, and W. Yao, Phys. Rev. Lett. **108**, 196802 (2012).
[12] X. Xu, W. Yao, D. Xiao, and T. F. Heinz, Nat. Phys. **10**, 343 (2014).
[13] B. Zhu, H. Zeng, J. Dai, Z. Gong, and X. Cui, Proc. Natl. Acad. Sci. U.S.A. **111**, 11606 (2014).
[14] A. M. Jones, H. Yu, J. S. Ross, P. Klement, N. J. Ghimire, J. Yan, D. G. Mandrus, W. Yao, and X. Xu, Nat. Phys. **10**, 130 (2014).
[15] S. Wu *et al.*, Nat. Phys. **9**, 149 (2013).
[16] H. Zeng, J. Dai, W. Yao, D. Xiao, and X. Cui, Nat. Nanotechnol. **7**, 490 (2012).
[17] Z. Gong, G.-B. Liu, H. Yu, D. Xiao, X. Cui, X. Xu, and W. Yao, Nat. Commun. **4**, 2053 (2013).
[18] X. Zhang, Q. Liu, J.-W. Luo, A. J. Freeman, and A. Zunger, Nat. Phys. **10**, 387 (2014).
[19] G. Kresse and J. Furthmüller, Comput. Mater. Sci. **6**, 15 (1996).
[20] G. Kresse and D. Joubert, Phys. Rev. B **59**, 1758 (1999).
[21] See Supplemental Material at http://link.aps.org/supplemental/10.1103/PhysRevLett.114.087402 for the derivation of Eq. (6), three kinds of other relaxation channels, possible reasons for the deviation between theory and experiment, and supplemental figures, as well as Refs. [22–28].
[22] H. Ochoa and R. Roldán, Phys. Rev. B **87**, 245421 (2013).
[23] H.-Z. Lu, W. Yao, D. Xiao, and S.-Q. Shen, Phys. Rev. Lett. **110**, 016806 (2013).
[24] D. Lagarde, L. Bouet, X. Marie, C. R. Zhu, B. L. Liu, T. Amand, P. H. Tan, and B. Urbaszek, Phys. Rev. Lett. **112**, 047401 (2014).
[25] T. Cao *et al.*, Nat. Commun. **3**, 887 (2012).
[26] P. Koskinen, I. Fampiou, and A. Ramasubramaniam, Phys. Rev. Lett. **112**, 186802 (2014).
[27] P. Johari and V. B. Shenoy, ACS Nano **6**, 5449 (2012).
[28] J. Klimeš, D. R. Bowler, and A. Michaelides, Phys. Rev. B **83**, 195131 (2011).
[29] R. Suzuki *et al.*, Nat. Nanotechnol. **9**, 611 (2014).
[30] J. M. Riley *et al.*, Nat. Phys. **10**, 835 (2014).
[31] L. Dong, A. M. Dongare, R. R. Namburu, T. P. O'Regan, and M. Dubey, Appl. Phys. Lett. **104**, 053107 (2014).
[32] We noted that the calculated circular polarization does not change if the MX_2 layers are slightly shifted or rotated relative to each other.
[33] G.-H. Lee *et al.*, ACS Nano **7**, 7931 (2013).
[34] C. L. Heideman, S. Tepfer, Q. Lin, R. Rostek, P. Zschack, M. D. Anderson, I. M. Anderson, and D. C. Johnson, J. Am. Chem. Soc. **135**, 11055 (2013).